Spectroscopic observation of the preferentially stabilized, linear He···ICl (X 1 Σ +) complex

Matthew D. Bradke and Richard A. Loomis

Citation: The Journal of Chemical Physics **118**, 7233 (2003); doi: 10.1063/1.1562622
View online: http://dx.doi.org/10.1063/1.1562622
View Table of Contents: http://scitation.aip.org/content/aip/journal/jcp/118/16?ver=pdfcov
Published by the AIP Publishing

Spectroscopic observation of the preferentially stabilized, linear He···ICl($X\,^1\Sigma^+$) complex

Matthew D. Bradke and Richard A. Loomis[a)]
Department of Chemistry, Washington University, CB 1134, St. Louis, Missouri 63130

(Received 7 January 2003; accepted 31 January 2003)

Spectroscopic features attributed to rovibronic transitions from both the T-shaped and linear He···$I^{35}Cl(X)$ and He···$I^{37}Cl(X)$ ground-state complexes have been recorded in the ICl $B\,^3\Pi_{0+}-X\,^1\Sigma^+$, 2–0 and 3–0 spectral regions using laser-induced fluorescence spectroscopy. Experiments performed using varying expansion conditions indicate that the He···$I^{35,37}Cl(X)$ complex with a linear equilibrium orientation lies lower in energy than the separately localized T-shaped isomer even though the transition energies of the T-shaped and linear complexes are shifted by ~3.5 and ~14 cm^{-1} to higher energy than the $I^{35,37}Cl$ $B-X$ band origins, respectively. Based on comparison with the excited state theoretical predictions of Waterland *et al.* [J. Chem. Phys. **92**, 4261 (1990)], estimates of the binding energies for the ground state T-shaped and linear He···$I^{35}Cl(X)$ complexes are 17 and 21 cm^{-1}, respectively, in qualitative agreement with the recently published predictions of 15.2 and 18.3 cm^{-1} obtained using high level *ab initio* theory for the ground state potential energy surface [J. Chem. Phys. **117**, 7017 (2002)]. © *2003 American Institute of Physics.* [DOI: 10.1063/1.1562622]

I. INTRODUCTION

The weakly-bound complexes comprised of diatomic halogens and rare gas, Rg, atoms have proven to be prototypical systems for studying long-range intermolecular forces, unimolecular reaction dynamics, and energy redistribution mechanisms.[1–3] The changes in the interactions within the complexes due to the masses, electron densities, and polarizabilities of the atom and molecule constituents have been systematically investigated by varying the rare gas atom within the complex, from He through Xe, and the dihalogen molecule, from I_2, Br_2, Cl_2, IBr, ICl, through ClF.[2] A strong agreement between experimental observations and theoretical predictions, especially in recent times, has strengthened the understanding of the dominant forces that exist within most of these weakly-bound complexes. Unfortunately, the comparisons between theoretical and experimental data are restricted since spectroscopy and dynamics experiments on the Rg–dihalogen systems tend to access only a limited range of intermolecular orientations and energies within the complexes.[2,3] For instance, the rovibronic spectroscopy of the Rg–dihalogen complexes in the $A\leftarrow X$ and $B\leftarrow X$ electronic band regions of the halogen tends to be preferentially sensitive to the excitation of ground state complexes with equilibrium T-shaped orientations. Microwave studies, on the other hand, most often probe rovibrational transitions of the linear isomer within the lowest vibrational level of the dihalogen in the ground electronic state.

It is desirable to obtain experimental data for Rg–dihalogen complexes that characterize multiple intermolecular vibrational levels that sample varying regions of the intermolecular potential. This data can in turn be used to more thoroughly test the accuracy of the results obtained from advancing theoretical methods. The experimental results reported here on the rovibronic spectroscopy of He···ICl complexes reveal that laser-induced fluorescence (LIF) features attributed to transitions of the separately stabilized T-shaped and linear isomers of the He···$I^{35}Cl(X)$ and He···$I^{37}Cl(X)$ complexes can be observed in the ICl $B-X$ spectral region with rotational resolution, breaking the trends that are typical for Rg–dihalogen clusters.[2,3] Furthermore, the transitions of the more strongly-bound linear isomers access different intermolecular vibrational levels within the He $+I^{35,37}Cl(B,v')$ excited states than do transitions of the T-shaped isomer. The experimental LIF spectra should provide a more stringent test for theoretical predictions of intermolecular potential energy surfaces, eigenvalues, and eigenfunctions, since both the T-shaped and linear regions of the $He+I^{35,37}Cl(X,v''=0)$ and of the $He+I^{35,37}Cl(B,v')$ potential surfaces are sampled by the He···$I^{35,37}Cl$ transitions in these spectra.

II. BACKGROUND

The increased accuracy of the theoretical methods that are currently available for characterizing the long-range interactions between Rg atoms and dihalogen molecules within their ground electronic states has developed a general understanding of the overall shape of the intermolecular potentials that is fairly well accepted.[2–4] For Rg–homonuclear dihalogen complexes, Rg···X_2, potential minima are expected in regions with the rare gas atom sampling the linear or end-on configuration relative to the diatomic molecule and another minimum in the T-shaped or side-on orientation. The relative depths of the potential wells, as well as the internuclear distances along which the wells are located, are dictated by a

a)Author to whom correspondence should be addressed.

number of factors including van der Waals attraction and exchange repulsion between the electron density of the dihalogen molecule and the rare gas atom.[2] The ground electronic state of the dihalogens is a $^1\Sigma^+$ state, and as a result, the potential energy between the dihalogen and the Rg atom in the linear orientation is predicted to be more attractive than that in the T-shaped orientation.

The interactions within Rg–heteronuclear dihalogen complexes are slightly different than those within the Rg–homonuclear dihalogen complexes because of the influences of the asymmetric electron distributions and, to some extent, the dipole-induced dipole forces arising from the permanent dipole moment of the heteronuclear dihalogens.[2,3,5] Up to three wells with varying depths are anticipated for the heteronuclear complexes with the deepest well being in the Rg$\cdots X-Y$ orientation, where X is the larger, more polarizable halogen atom.[5] The relative depths of the two remaining wells, one in the near T-shaped and the other in the antilinear Rg$\cdots Y-X$ orientations, and the heights of the barriers between the wells and how to experimentally sample these regions remain interesting issues.

Both the zero-point energy and the vibrational energy localized in the intermolecular motions of the weakly-bound complexes will dictate the regions of the multidimensional potential energy surfaces that are sampled by the Rg-atom around the dihalogen molecule. While the linear well is expected to be the global minimum for each ground state potential energy surface,[2] the surface is quite anharmonic in this region and there is a correspondingly higher amount of zero-point energy in the linear orientations in comparison with that in the slightly more isotropic T-shaped region. The linear complexes also have an additional vibrational degree of freedom over the nonlinear geometries, resulting in a further increase in the amount of zero-point energy in the linear orientation. In order to predict what geometries and motions will be prominent within the ground state for each specific Rg–dihalogen complex, the following related questions must be addressed and answered. Does the combination of the increased zero-point energy in the linear orientation and the pairwise additive attraction in T-shaped geometries localize the ground state complex as T-shaped? Or, is the potential in the linear orientation attractive enough and are the barriers to rotation of the rare gas atom about the dihalogen large enough to localize the ground state complex in a linear geometry? Or, are there multiple regions of the potential along which the rare gas atom can be localized, resulting in stable linear, T-shaped, and perhaps antilinear ground state isomers? Or lastly, are the effective ground state potential energy surfaces isotropic to the point that the rare gas atom samples all orientations and is delocalized with respect to the dihalogen?

Numerous spectroscopic investigations using an array of experimental techniques have been undertaken to determine the answers to the preceding questions and the equilibrium structures of the weakly-bound, ground state Rg–dihalogen complexes.[3,4] Since a number of review articles have described the details and conclusions drawn from many of these studies, we generalize the trends that have been reported: Rovibronic spectroscopy experiments that access intermolecular levels correlating with the electronically excited dihalogens with vibrational excitation usually reveal T-shaped structures for the ground state complexes. The ground state structures are determined to be linear in most microwave investigations. A few of the Rg–dihalogen systems lie outside of these trends and warrant brief comments.

Distinct intermolecular vibrational bands, appearing as satellite features to higher transition energies of each I_2 vibrational band, as well as a broad, structureless continuum signal were observed in the LIF spectra of Ar$\cdots I_2$ throughout the I_2 $B-X$, v'-0 region.[4,6,7] The rotational structure of the discrete bands could be partially resolved when utilizing high-resolution lasers and could be fit with ground and electronically excited state rigid-rotor constants corresponding to equilibrium T-shaped geometries. The lifetimes of the T-shaped Ar$\cdots I_2(B,v')$ complexes are short-lived in comparison to the fluorescence lifetime of the complex since vibrational predissociation of the complex is efficient and forms separate Ar atoms and electronically excited $I_2(B,v)$ molecules with less vibrational excitation than the excited state complex, $v<v'$. Transitions of complexes in this region are still observed in LIF spectra since the electronically excited dihalogen fragments, $I_2(B,v)$, relax via fluorescence. The observation of rovibronic bands attributed to transitions of the ground state T-shaped isomer to short-lived excited state levels at energies just higher than each monomer dihalogen band is the norm for most of the Rg–dihalogen systems investigated. The observation of the broad background signal, however, was quite significant. Although the origin of the diffuse signal has not been definitively determined, it has been proposed that transitions of the linear Ar$\cdots I_2(X)$ isomer in the I_2 $B-X$ region access a repulsive wall of the excited state potential energy surface.[6] Excited state complexes prepared on this region of the potential would quickly dissociate into $I_2(B,v)$ fragments. As a result, the fluorescence signals attributed to rovibronic transitions of the linear Ar$\cdots I_2(X)$ complexes in the $B-X$ region are lifetime broadened to the extent that the fluorescence features overlap and appear as a weak continuum signal. The spectroscopy experiments on Ar$\cdots I_2(X)$ not only indicate the existence of two separately stabilized, ground state isomers, a linear and a T-shaped complex, but also that the linear isomer was more strongly bound than the T-shaped.[6] A 3:1 population ratio of the linear to T-shaped ground state isomers at a temperature of $\sim$15 K was estimated in these experiments by comparing the total continuum signal to that of the discrete rovibronic bands of the T-shaped complexes.

As for Ar$\cdots I_2$ and most of the other Rg$\cdots$dihalogen complexes,[4,6,7] discrete rovibronic transitions from a linear Ne$\cdots I_2(X)$ isomer have not been observed in the $B-X$ spectral region when using LIF spectroscopy.[8,9] The results from double resonance and fluorescence depletion spectroscopy experiments performed on Ne$\cdots I_2$, also in the I_2 $B-X$ region, do indicate different ground and excited state interactions than for the Ar$\cdots I_2$ system.[9] Two laser, action spectroscopy experiments revealed several rovibronic spectral features attributable to a progression of intermolecular vibrational levels accessing the linear, T-shaped or both of the orientations within the electronically excited Ne$+I_2(B,v')$

wells that were not observed in the corresponding LIF spectra. Fluorescence depletion experiments determined that all of the different excited state levels were accessed by transitions originating from the same ground state $Ne\cdots I_2(X,v''=0)$ intermolecular level. The conclusion concerning the geometry of the ground state $Ne\cdots I_2(X)$ complex is that the Ne atom is delocalized with respect to the $I_2(X)$ molecule and ground state isomers with distinct equilibrium orientations are not stabilized.

Two spectral features attributed to rovibronic transitions of $He\cdots Br_2$ complexes were observed to higher energy of each vibrational band in the $Br_2\,B-X$ spectral region using two-laser pump–probe spectroscopy.[10] The resolution of the excitation laser was such that distinctly different rotational contours were observed for the two bands, with the lower energy features having distinct *R*-branch bandheads and the higher-energy features spanning a larger energy region with no distinct bandheads. The lower energy features were attributed to transitions of the T-shaped $He\cdots Br_2(X)$ complexes to the lowest intermolecular vibrational level with an equilibrium T-shaped geometry lying within each $He+Br_2(B,v')$ well. The higher-energy features were originally assigned as transitions of the T-shaped complexes to excited state levels of the $He\cdots Br_2(B,v')$ complex with at least one quanta of intermolecular vibrational excitation. Subsequent theoretical predictions[11] indicate that the higher-energy features are more likely that of a separately stabilized $He\cdots Br_2(X)$ complex with an equilibrium linear geometry to excited state levels with intermolecular vibrational excitation.

The microwave spectra of the He···ClF complex, which contains features attributed to direct rovibrational transitions between intermolecular levels with T-shaped and linear equilibrium structures, also break the trends thus far observed for Rg–dihalogen complexes.[5] The difference in energy between the more stable linear state and the higher-energy T-shaped $He\cdots{}^{35}ClF$ state was observed to be only 2.320 cm^{-1}. Accompanying calculations of the $He+ClF(X)$ ground state potential energy surface predicted a significantly larger difference, 22.9 cm^{-1} between the depths of the linear and T-shaped wells. The effect of zero point vibration on the binding energy of the highly nonrigid, weakly-bound $He\cdots ClF(X)$ complex is clearly exhibited since the large, additional amount of zero point energy in the linear region of the potential energy surface over that in the T-shaped region is comparable to the difference in the well depths for the linear and T-shaped orientations.[5]

The larger dipole moment of ICl(X), 1.207 D,[12] vs ClF(X), 0.8881 D,[5] suggests that the dipole-induced dipole forces between ICl and He in $He\cdots ICl(X)$ complexes should be even stronger than between He and ClF. The dipole moment of ICl may also give rise to contributions from charge transfer between the highly polarizable I-atom and the He-atom in the intermolecular interactions. The $He\cdots ICl(X)$ complexes may therefore have a propensity for stronger attraction in the linear geometry as compared to that in the near T-shaped orientation. Although other larger, more polarizable Rg atoms should be more strongly bound to ICl(X) than He atoms, the use of a He-atom as a complex partner offers several advantages. A helium expansion permits high backing pressures to be utilized and thus low translational, rotational, and to some extent vibrational temperatures to be achieved within the expansion without significant complications arising from higher-order Rg_n or $Rg_n\cdots ICl(X)$, $n>1$, clusters.[13] The large deBroglie wavelength of the He atom and the corresponding quantum effects in helium supersonic expansions also lower the ultimate temperatures that can be achieved in comparison to the heavier Rg atoms.[13,14]

The previously reported LIF spectra of T-shaped $He\cdots ICl(X)$ complexes in the ICl $B-X$, 2–0 and 3–0 regions that were recorded during experiments aimed at characterizing the excited state vibrational predissociation dynamics of $He\cdots ICl(B,v'=2,3)$ complexes[15–18] served as a foundation for the spectroscopic efforts reported here. The published He···ICl LIF spectra were recorded using modest backing pressures with a continuous, free-jet expansion that cooled the ICl(X) molecules to rotational temperatures on the order of 2 K.[15] Under those conditions, the T-shaped $He\cdots I^{35,37}Cl$ LIF spectral features were observed as satellite features shifted just to higher energy than the corresponding $I^{35,37}Cl\,B-X$ transitions. Vibrational predissociation of the excited state $He\cdots I^{35}Cl(B,v')$ complexes was found to form $He+I^{35}Cl(B,v'\text{-}1)$ fragments, which in turn fluoresce. In the present study, we have recorded the LIF spectra of He···ICl complexes in the ICl $B-X$ spectral region using more severe expansions conditions than used in the previous reports. By systematically varying the expansion conditions and comparing the LIF spectra recorded using each set of conditions, we have not only identified new features that we attribute to transitions from the linear $He\cdots I^{35,37}Cl(X)$ isomers, but we have also verified that the linear ground state isomer is more strongly bound than the T-shaped complexes.

III. EXPERIMENT

The ground state $He\cdots ICl(X)$ complexes were stabilized within a pulsed supersonic expansion. A helium carrier gas, with a pressure fixed between 15 and 315 psi relative to vacuum, flowed through a sample vessel containing solid ICl maintained at a well-defined temperature between 274 and 298 K with an accuracy of 1 K. Varying the temperature of the ICl sample controlled the partial pressure of the ICl with a fixed total backing pressure within the expansion. Low sample temperatures proved effective in minimizing the presence of molecular iodine vapor, a decomposition product of ICl, within the expansion; I_2 has a vapor pressure of ~0.05 Torr at 273 K (Ref. 19) versus 3.69 Torr for ICl.[20] The minimization of molecular iodine in the expansion was a necessity since the $I_2\,B-X$ LIF spectrum spans the entire ICl $B-X$ spectral region and thus could overlap the weaker ICl LIF features of interest. The data presented here were recorded with the ICl sample held at 274 K unless otherwise stated. The He/ICl mixture was pulsed at 10 Hz through an 800 μm diam nozzle into the vacuum chamber, which was maintained at pressures below 20 mTorr during an experiment using a roots blower mechanical pumping system with a speed of ~1900 l/s.

Laser-induced fluorescence spectra were recorded throughout the ICl $B-X$, 1–0, 2–0, and 3–0 spectral regions, between 558 and 573 nm, using a commercial

Nd:YAG pumped dye laser operating with rhodamine 6G dye. The laser beam was gently focused using a 1 m lens to a spot size of ~3 mm in the supersonic expansion region at distances centered between 4.0 and 14.0±0.5 mm from the pulsed valve orifice. These distances correspond to reduced distances x/d, defined by the distance downstream divided by the nozzle diameter, of 5.0–17.5. Survey scans aimed at locating spectral features attributed to transitions of the He···ICl complexes and at optimizing the expansion conditions required for formation of the complexes were performed using the dye laser operating with low frequency resolution, 0.22 cm^{-1}, and with pulse energies between 25 and 30 mJ/pulse measured within the chamber. High-resolution LIF spectra were also recorded by placing an intracavity étalon within the oscillator cavity of the dye laser. A resolution of 0.06–0.08 cm^{-1}, depending on the wavelength, was achieved with a pulse energy of 5–7 mJ/pulse within the chamber. The frequency of the dye laser could be scanned over ~7 cm^{-1} windows by initially pressurizing the oscillator cavity with ~2 atm of dry nitrogen and then releasing the nitrogen out of the cavity through a small manual leak valve.

Resultant fluorescence was collected with an F/1 mirror and telescope assembly and imaged onto a visible wavelength photomultiplier tube. A 10 mm×4 mm rectangular mask with the long axis oriented parallel to the direction of the expansion was positioned within the telescope assembly so that only fluorescence from the centermost region of the expansion was collected. A combination of 600 and 610 nm long-pass filters was placed before the photomultiplier tube to block laser scatter and to transmit fluorescence in the ICl $B \rightarrow X$ Franck–Condon window.[21] Two boxcar gated integrators were used to record the intensity of the LIF signal as a function of laser excitation wavelength. One integration gate with a width of 500 ns was set at long time, ~100 ns after the excitation laser, to collect fluorescence from long-lived excited state species. A second narrow gate, 10 ns, was set at short time, directly over the excitation laser, to preferentially monitor fluorescence from short-lived excited-state species within the expansion, e.g., ICl($B, v'=3$) monomers. A small fraction of the excitation light was passed through an iodine sample optical cell and was transmitted through a solid étalon with a free spectral range of 2.2 cm^{-1} and a finesse of 100 in order to calibrate the excitation wavelength in the spectral scans.

Dispersed fluorescence experiments were performed by replacing the photomultiplier with a 0.32 m monochromator. The fluorescence was collected from the laser-interaction region using the same telescope assembly with the mask removed and was imaged onto the entrance slit of the monochromator using an F/4 spherical lens. A liquid nitrogen-cooled CCD array with a 568×356 pixel plane was used to record the dispersed fluorescence spectra with a typical resolution of ~6 cm^{-1}.

IV. RESULTS

A. Laser-induced fluorescence survey spectra

Low-resolution LIF spectra were recorded in the ICl $B-X$, 1–0, 2–0, and 3–0 spectral regions using helium backing pressures between 15 and 315 psi. Multiple satellite features are observed in each spectral region just to higher energy than the well-characterized vibrational bands of the $I^{35}Cl$ and $I^{37}Cl$ molecules.[22–25] The satellite features are attributed to transitions of the weakly-bound He···$I^{35,37}Cl(X)$ complexes to intermolecular vibrational levels correlating with the He+$I^{35,37}Cl(B, v'=1,2,3)$ asymptotes. The fluorescence excitation spectra of the He···ICl complexes are most easily recorded in the ICl $B-X$, 3–0 spectral region since the Franck–Condon factors for the 3–0 transitions are the largest within the $B-X$ region that can be accessed.[21] Furthermore, while the ICl $B-X$, v'-0 monomer vibrational bands have energies that to some extent overlap the He···ICl spectral features, the curve crossing of the purely dissociative ICl($Z1$) state with the ICl($B\,^3\Pi_{0+}$) potential well near the $v'=3$ level greatly reduces the excited state lifetime of the ICl($B, v'=3$) rotational states and the fluorescence quantum yield when promoting ICl molecules to these states.[21,26–28]

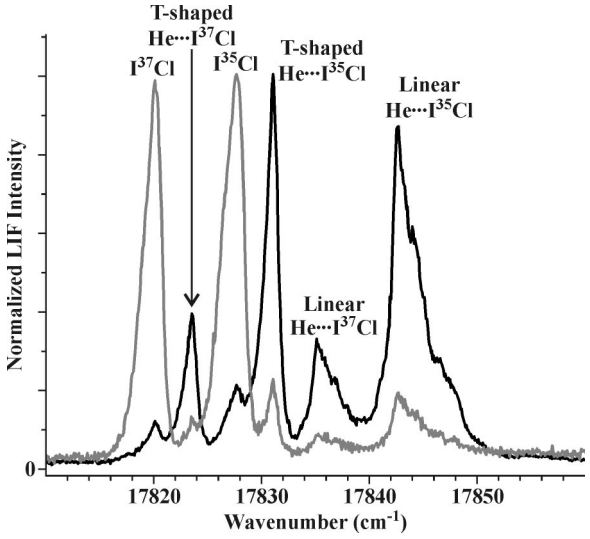

FIG. 1. Low-resolution (~0.2 cm^{-1}) LIF spectra recorded in the ICl $B-X$, 3–0 spectral region. The spectra were recorded with a 115 psi helium backing pressure, with the laser interesecting the expansion at $x/d=12.5$, and with one boxcar integration gate placed at short time (gray line) and another at long time (black line) to preferentially probe transitions attributed to the ICl monomers and the He···ICl complexes, respectively. The intensities of the spectra were normalized to be the same.

The LIF spectra recorded in the ICl $B-X$, 3–0 spectral region shown in Figure 1 were collected using a helium backing pressure of 115 psi with the laser axis intersecting the supersonic expansion at $x/d=12.5$. The gray spectrum was recorded using a boxcar integration gate positioned at short time and is dominated by the $I^{37}Cl$ and $I^{35}Cl$ monomer bands at 17 820 and 17 827 cm^{-1}, respectively, that access the short-lived $I^{35,37}Cl(B, v'=3)$ rotational states.[26,27,29] The four significantly weaker features, at 17 824, 17 831, 17 835, and 17 842 cm^{-1}, are attributed to rovibronic transitions of He···$I^{35,37}Cl$ complexes. The black spectrum in Fig. 1, obtained using a gate positioned at long time, shows an enhancement of the intensities of these four bands over that of the $I^{35,37}Cl$ $B-X$, 3–0 monomer bands. This is because of the significantly longer fluorescence decay profile observed for these bands (microseconds) in comparison to the short

lifetimes of the monomer bands (less than the 8 ns laser pulse width). The lower energy He···$I^{35,37}Cl$ rovibronic bands at 17 824 and 17 831 cm^{-1} have been observed previously[15,30] and are attributed to transitions of the He···$I^{37}Cl(X)$ and He···$I^{35}Cl(X)$ complexes with equilibrium T-shaped geometries to bound intermolecular vibrational levels correlating with $He+I^{37}Cl(B,v'=3)$ and $He+I^{35}Cl(B,v'=3)$, respectively. In partial support of this assignment, the difference between the transition energies of the He···$I^{37}Cl$ and He···$I^{35}Cl$ T-shaped features, ~7 cm^{-1}, is approximately the same as the difference between the transition energies of the $I^{37}Cl$ and $I^{35}Cl\,B-X$, 3–0 bands, as would be expected for transitions of complexes comprised of the different ICl isotopes. In addition, the ratio of the intensities of these features, He···$I^{35}Cl$ to He···$I^{37}Cl$ T-shaped, is ~3:1, corresponding to the ratio of the $I^{35}Cl$ to $I^{37}Cl$ isotopic abundances.

Although the two remaining He···$I^{35,37}Cl$ features at 17 842 and 17 835 cm^{-1} were not observed previously, the transition energies of these two bands are also separated by ~7 cm^{-1} and the ratio of the band intensities is ~3:1. This supports the assignment that these spectral features are from rovibronic transitions of the He···$I^{35}Cl$ and He···$I^{37}Cl$ complexes that originate from levels with the same intermolecular vibrational excitation in the $He+I^{37}Cl(X,v''=0)$ and $He+I^{35}Cl(X,v''=0)$ ground states and terminate on the same levels in the $He+I^{37}Cl(B,v'=3)$ and $He+I^{35}Cl(B,v'=3)$ excited electronic states. The rotational contours of the newly observed features are significantly different than those for the rovibronic bands of the $I^{35,37}Cl(X)$ monomers and the T-shaped He···$I^{35,37}Cl(X)$ complexes, which exhibit distinct R-branch bandheads and appear to be rotationally cold as each feature has a breadth of <4 cm^{-1}. The higher-energy He···$I^{35,37}Cl$ features span broader energy regions, >7 cm^{-1}, with contours suggesting either no bandheads or possible P-branch bandheads with rotational structure extending toward higher transition energies.

The newly detected features are most likely not due to transitions of higher-order He_n···$I^{35,37}Cl(X)$ clusters since they are observed at $\sim+15$ cm^{-1} from the corresponding $I^{35,37}Cl\,B-X$, 3–0 monomer transition energies. The transition energies of higher-order Rg_n–dihalogen clusters observed previously follow a band shift rule, where the transition energy of a Rg_n–dihalogen cluster is observed at an energy of $\sim+n\Delta E$ from the dihalogen vibrational band where $+\Delta E$ is the difference in energy between the band of the Rg–dihalogen complex and the dihalogen vibrational band.[8,31] Following the band shift rule, the transitions of the He_2···$I^{37}Cl$ and He_2···$I^{35}Cl$ clusters would be expected at $\sim+8$ cm^{-1} from the monomer bands or 17 828 and 17 835 cm^{-1}, respectively, not at 17 835 and 17 842 cm^{-1} as observed.

The very intense $I^{37}Cl$ and $I^{35}Cl$ LIF features at 17 659 and 17 664 cm^{-1} dominate the spectrum in the $ICl\,B-X$, 2–0 energy region. Three significantly weaker bands attributed to transitions of He···$I^{35,37}Cl$ complexes are observed to higher transition energies than the monomer features. The lowest energy feature with a peak intensity at 17 668 cm^{-1} was observed previously[15] and was attributed to excitation of the T-shaped He···$I^{35}Cl(X)$ complex to an intermolecular vibrational level lying within the $He+I^{35}Cl(B,v'=2)$ well. A similar feature attributed to rovibronic transitions from the He···$I^{37}Cl(X)$ complex could not be detected due to overlap of the intense $I^{35}Cl\,B-X$, 2–0 band in the expected energy region. The two remaining LIF features observed at higher transition energies, 17 673 and 17 678 cm^{-1}, are attributed to transitions of He···$I^{37}Cl(X)$ and He···$I^{35}Cl(X)$ complexes, respectively. The energy between these two bands, ~5 cm^{-1}, being consistent with the energy spacing between the $I^{37}Cl$ and $I^{35}Cl\,B-X$, 2–0 monomer bands and the ~3:1 intensity ratio for the 17 678 cm^{-1} to 17 673 cm^{-1} features matching the 3:1 isotopic ratio supports this assignment.

LIF spectra were also recorded in the $ICl\,B-X$, 1–0 region. All of the features in this region are very weak due to the small Franck–Condon factors for these transitions[21] and the transition energies lying on the edge of the rhodamine 6G dye curve. In addition to the two monomer rovibronic bands, three LIF features lying to higher energy are observed and are attributed to transitions of He···$I^{35,37}Cl$ complexes. The lowest energy He···ICl feature in this region is attributed to rovibronic transitions of the T-shaped He···$I^{35}Cl(X)$ complex and the two higher energy, previously unreported features to transitions of the He···$I^{37}Cl$ and He···$I^{35}Cl$ complexes following the trends observed in the 2–0 and 3–0 regions. The overall weakness of the signal intensities associated with these complex bands made careful interrogation and characterization of these features difficult and as a consequence they have not been investigated further.

B. Dependence of signals on source conditions

In order to verify that the newly detected LIF features arise from rovibronic transitions of the He···$I^{35,37}Cl(X)$ complexes and to possibly identify the intermolecular vibrational levels accessed in these excitation bands, LIF spectra were recorded using varying He backing pressures, distances downstream in the expansion, and ICl partial pressures. For a given set of source parameters, a LIF spectrum was recorded in the 3–0 region so that the intensity of each He···$I^{35,37}Cl$ spectral feature could be monitored and a LIF spectrum of the $I^{35}Cl\,B-X$, 2–0 rovibronic band was acquired to provide a relative scaling factor for the intensities of the He···$I^{35,37}Cl\,B-X$, 3–0 spectral features.

LIF spectra were recorded using varying helium backing pressures, 15–85 psi, with the ICl sample reservoir held at 274 K and the laser intersecting the supersonic expansion at $x/d=12.5$. Since each of the features attributed to transitions of the He···$I^{35,37}Cl(X)$ complexes in the $ICl\,B-X$, 3–0 region overlap to some extent other He···ICl features or molecular ICl bands, the integrated intensity of each He···ICl band could not be determined without introducing significant error. The peak intensities of each of the He···ICl bands, the T-shaped He···$I^{37}Cl$ and He···$I^{35}Cl$ bands at 17 824 and 17 831 cm^{-1} and the higher-energy He···$I^{37}Cl$ and He···$I^{35}Cl$ bands at 17 835 and 17 842 cm^{-1}, were therefore measured for each backing pressure. The peak intensities of the complexes were normalized to 0.001 times that of the $I^{35}Cl\,B-X$,

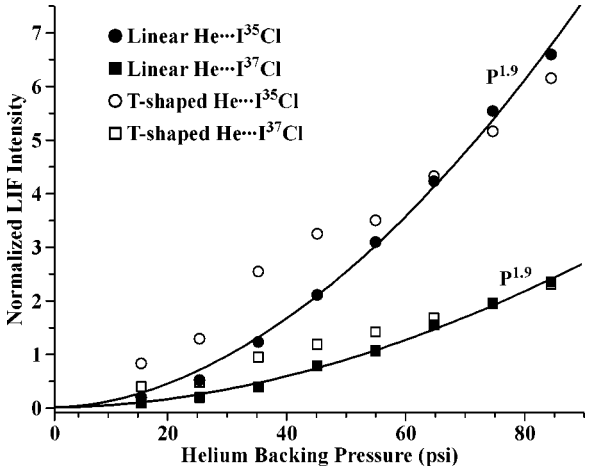

FIG. 2. Helium backing pressure dependence of the peak intensities of the He···ICl LIF features recorded in the ICl $B-X$, 3–0 spectral region (□, 17 824 cm^{-1}; ○, 17 831 cm^{-1}; ■, 17 835 cm^{-1}; ●, 17 842 cm^{-1}). The intensities of the bands are normalized to 0.001× the intensity of the $I^{35}Cl$ $B-X$, 2–0 band at each pressure. Fits of the peak intensities of the higher-energy features (filled symbols, ■ and ●) follow nearly a pressure-squared dependence, indicative of a binary He···ICl(X) complex formed via three-body collisions. The T-shaped bands (open symbols, □ and ○) do not follow a single power dependence on pressure over the range investigated.

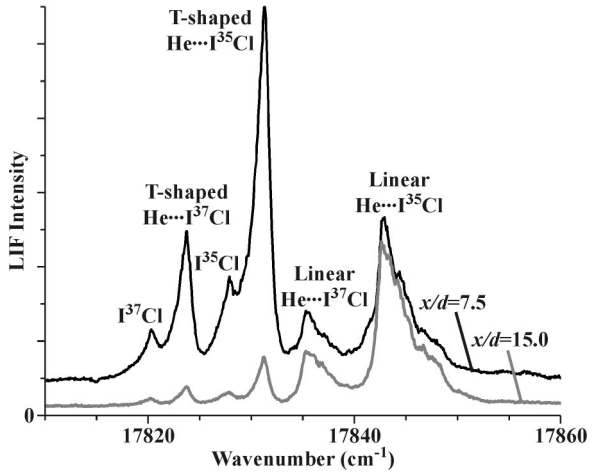

FIG. 3. Low-resolution (~0.2 cm^{-1}) LIF spectra recorded in the ICl $B-X$, 3–0 spectral region at reduced distances of 7.5 and 15.0 using 115 psi of He backing pressure with the ICl sample at 274 K. The spectra are plotted on the same vertical scale to permit direct comparison of the intensities. High-resolution (~0.06 cm^{-1}) LIF spectra of the $I^{35}Cl$ $B-X$, 2–0 monomer feature were also recorded with these conditions (not shown) and the rotational contours were best simulated using rotational temperatures of 3.1 and 1.4 K at the 7.5 and 15.0 reduced distances, respectively.

2–0 band and are plotted in Fig. 2 as a function of the He backing pressure.

The ~3:1 ratio of the intensities of the T-shaped He···$I^{35}Cl$ to He···$I^{37}Cl$ features and of the higher-energy He···$I^{35}Cl$ to He···$I^{37}Cl$ features was maintained throughout the pressure region covered. A fit of the peak intensities of the higher-energy features versus He backing pressure, P, raised to a single algebraic power revealed a $P^{1.9}$ dependence at these modest backing pressures, ≤85 psi. This pressure dependence represents further evidence for assigning the two newly observed higher-energy LIF features to transitions of He···$I^{37}Cl(X)$ and He···$I^{35}Cl(X)$ complexes rather than He_n···ICl(X) higher-order clusters since a P^2 dependence is expected for the stabilization of Rg···XY complexes via three body collisions and a P^4 dependence is expected for the stabilization of higher-order Rg_2···XY complexes.[31] The intensities of the T-shaped features appear to have a more complicated dependence on helium backing pressure and could not be fit to a single power-dependence over this pressure range. The T-shaped features are more intense than the higher-energy bands at the lower backing pressures and then have a more gentle dependence on backing pressure, becoming less intense than the higher-energy features at backing pressures above 65 psi.

The dependence of the relative intensities of the different He···ICl LIF features on the local rotational temperature and the number of collisions within the expansion was investigated by recording spectra in the 3–0 region at varying distances downstream from the pulsed valve. Low-resolution LIF spectra were recorded using a He backing pressure of 115 psi and with the ICl sample reservoir held at 274 K at three different distances, $x/d=7.5$, 11.3, and 15.0. A high-resolution spectrum of the $I^{35}Cl$ $B-X$, 2–0 rovibronic band was recorded immediately after acquiring the low-resolution spectrum at each distance. A fit of the high-resolution $I^{35}Cl$ spectrum indicated rotational temperatures $T_{rot}=3.1(2)$, 1.9(2), and 1.4(1) K at the three distances, respectively. The ICl monomer bands, the four He···ICl bands as well as the continuum fluorescence signal spanning the entire ICl $B-X$, 3–0 energy region are observed in the LIF spectra that were recorded at the three distances. The low-resolution spectra for the $x/d=7.5$ and 15.0 distances are shown in Fig. 3 with both spectra plotted on the same vertical scale. The relative intensities of the T-shaped He···$I^{35}Cl(X)$ to He···$I^{37}Cl(X)$ features and the higher-energy He···$I^{35}Cl(X)$ to He···$I^{37}Cl(X)$ features maintain the ~3:1 isotopic abundance ratio in each of the three spectra. The intensities of the T-shaped He···ICl bands are greater than the higher-energy bands at the shortest distance with a rotational temperature of 3.1 K. At $x/d=11.3$, not shown, the intensity of the T-shaped and higher-energy He···ICl features containing each isotope are comparable. The higher-energy features become more intense than the lower energy, T-shaped He···ICl features further downstream ($x/d=15.0$) where a rotational temperature of 1.4 K was determined.

Lastly, low-resolution LIF spectra were recorded using varying temperatures of the ICl sample reservoir, thereby changing the partial pressures of ICl in the expansion, to rule out the possibility of detecting features attributable to He···$ICl_n(X)$ complexes with $n>1$. The LIF spectra of the complexes in the 3–0 spectral region and of the $I^{35}Cl$ 2–0 monomer band were recorded with a fixed He backing pressure, 115 psi, and with the laser crossing the supersonic expansion at $x/d=12.5$. The ICl sample temperature was varied from 274 to 298 K in increments of 3 K so that the LIF spectra could be acquired with the ICl partial pressure increasing by nearly a factor of 4.[20] The relative intensities of the ICl $B-X$, 2–0 monomer, and all four of the He···ICl $B-X$, 3–0 LIF features all scaled with each other as the ICl partial pressure was varied. Furthermore, no addi-

tional features attributable to transitions of species containing ICl were observed with the higher ICl partial pressures, suggesting that clusters with more than one ICl molecule are not formed under these conditions.

Two conclusions can be drawn from these systematic studies. First, the ground state He···$I^{35}Cl(X)$ and He···$I^{37}Cl(X)$ complexes can be stabilized in different intermolecular vibrational levels, perhaps sampling different equilibrium geometries representing different isomers of the He···$I^{35,37}Cl(X)$ complexes. Rovibronic transitions from the different He···$I^{35,37}Cl(X)$ ground state levels give rise to the T-shaped and the higher-energy LIF features in each ICl $B-X$, v'-0 region. Second, the He···$I^{35,37}Cl(X)$ intermolecular vibrational levels that give rise to the higher-energy LIF features are more strongly bound than the T-shaped He···$I^{35,37}Cl(X)$ levels since they are preferentially populated at lower temperatures. The lowest energy He···ICl$(X,v''=0)$ intermolecular vibrational level is most likely that of the linear isomer based on expectations for Rg–heteronuclear dihalogen complexes.[2,4,5]

C. High-resolution spectra

High-resolution LIF spectra of the T-shaped and of the higher-energy He···ICl bands were recorded in the ICl $B-X$, 2–0 and 3–0 spectral regions in an attempt to determine the ground and excited state equilibrium structures of the levels accessed in each of the He···$I^{35,37}Cl(X)$ rovibronic bands. The spectra were recorded using a He backing pressure of 215 psi and with the excitation laser intersecting the expansion at $x/d=12.5$ so that the intensities of the T-shaped and higher-energy He···ICl bands for each ICl isotope were of comparable intensity. Since the dye laser could only be used to record a high-resolution spectrum over a limited range in a single scan, <7 cm^{-1}, the high-resolution LIF spectra spanning the ICl $B-X$, 2–0 and 3–0 regions had to be generated by piecing together multiple scans covering neighboring transition energy windows. The high-resolution LIF spectrum shown in Fig. 4 was recorded in the ICl $B-X$, 3–0 region and represents the sum of six spectra, each recorded over a 4–7 cm^{-1} window. The different spectra were recorded consecutively with each spectral window overlapping the transition energy of the neighboring regions so that a consistency in the intensity scale could be maintained across the $\sim$40 cm^{-1} region. An average of three scans, representing a total of 30 laser shots per data point, were recorded for each window.

Inspection of the individual He···ICl $B-X$, 2–0 and 3–0 rovibronic bands reveals distinct differences between the overall rotational structure of the LIF features attributed to transitions of the T-shaped He···$I^{35,37}Cl(X)$ and the other energetically more stable He···$I^{35,37}Cl(X)$ complexes, Fig. 5. The contour of the T-shaped features, as shown in panel (c), is consistent with those reported previously by the Lester group[15,30] with a distinct bandhead on the R-branch and only a few rotational lines observed. The higher-energy features are drastically different with a P-branch bandhead possible and a larger number of rotational lines resolved extending to higher transition energy, panels (a) and (b). The rotational structure of the features in the ICl $B-X$, 2–0 and 3–0 regions are qualitatively similar with each band having a comparable number of rotational lines occurring at approximately the same transition energies relative to the most intense feature within each band.

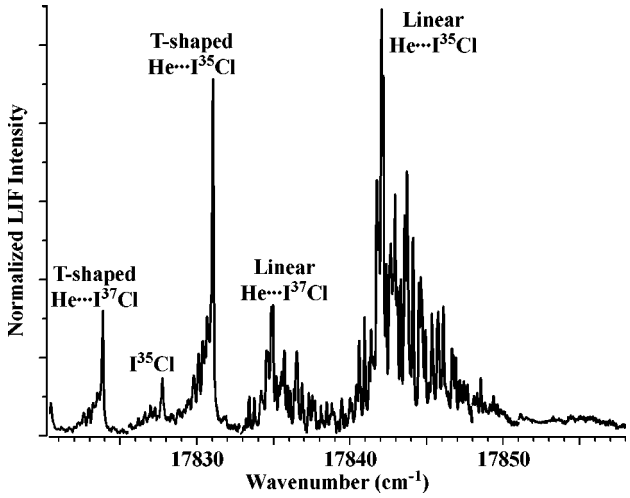

FIG. 4. High-resolution ($\sim$0.08 cm^{-1}) LIF spectrum recorded over the ICl $B-X$, 3–0 spectral region. Since the current apparatus limits the recording of high-resolution spectra to <7 cm^{-1} windows, the full spectrum was obtained by piecing together six different spectra with the intensity scale for each window normalized to common rotational lines on neighboring windows.

Rigid-rotor simulations of the rotational structure for each of the He···$I^{35,37}Cl$ LIF rovibronic bands were per-

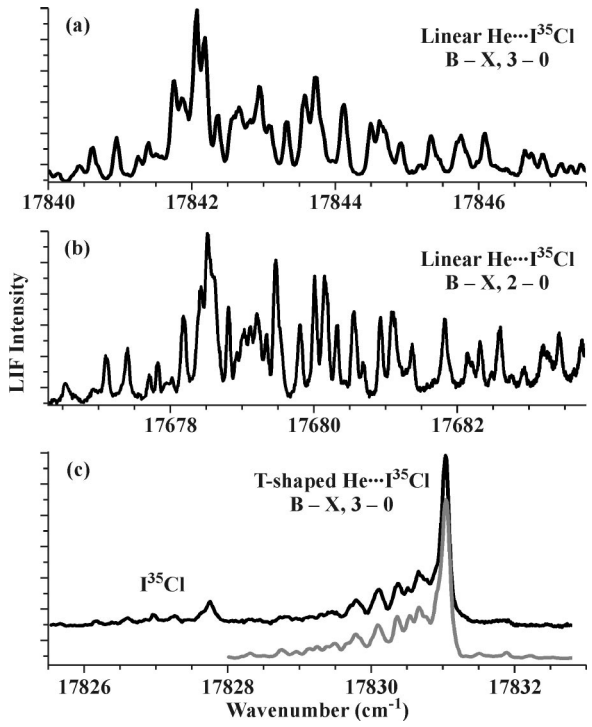

FIG. 5. High-resolution LIF features attributed to transitions of the He···$I^{35}Cl$ complexes in the ICl $B-X$ spectral region. The rotational contours associated with transitions of the linear He···$I^{35}Cl(X)$ isomer in the 3–0 and 2–0 regions, (a) and (b), respectively, are distinctly different than that of the T-shaped isomer, (c). The fit of the T-shaped He···$I^{35}Cl$ $B-X$, 3–0 rotational band contour is plotted as a gray spectrum offset below the experimental data.

TABLE I. Spectroscopic constants (in cm^{-1}) of the T-shaped He···ICl bands recorded in the ICl $B-X$, 2–0 and 3–0 spectral regions.

	He···I^{35}Cl 2–0		He···I^{35}Cl 3–0	He···I^{37}Cl 3–0
ν_0	17667.25 (4)	17667.3(1)[a]	17830.80 (3)	17823.64 (3)
A''	0.253(3)[b]	0.259[a]	0.253(3)[b]	0.263(4)
B''	0.111(3)[b]	0.114[a]	0.111(3)[b]	0.110(3)
C''	0.078(3)[b]	0.079[a]	0.078(3)[b]	0.077(4)
A'	0.234 (4)	0.237[a]	0.233 (3)	0.240(4)
B'	0.078 (5)	0.082[a]	0.080 (4)	0.078(3)
C'	0.058 (5)	0.061[a]	0.060 (3)	0.058(4)

[a]Spectroscopic constants reported previously (Ref. 30).
[b]The fitting of the T-shaped He···I^{35}Cl $B-X$, 2–0 and 3–0 bands were performed simultaneously, keeping the ground state constants the same for each band.

TABLE II. Transition energies (in cm^{-1}) of the He···ICl spectral features recorded in the ICl $B-X$, 2–0 and 3–0 spectral regions.

		I^{35}Cl		I^{37}Cl	
	Feature	Position	Shift	Position	Shift
	Monomer	17 664.08(1)	0	17 658.79(1)	0
$v'=2$	T-shaped[a]	17 667.25(4)	3.17	...[b]	...[b]
	Linear	17 678.4[c]	14.3	17 673.3[c]	14.5
	Monomer	17 827.49(2)	0	17 820.20(2)	0
$v'=3$	T-shaped[a]	17 830.80(3)	3.31	17 823.64(3)	3.44
	Linear	17 841.7[c]	14.2	17 834.5[c]	14.3

[a]The T-shaped features were observed previously (Refs. 15, 30) with band origins reported to be 17 667.4 cm^{-1} for the He···I^{35}Cl $B-X$, 2–0 band, 17 831.0 for the He···I^{35}Cl $B-X$, 3–0 band, and 17 823.9 cm^{-1} for the He···I^{37}Cl $B-X$, 3–0 band.
[b]The T-shaped He···I^{37}Cl $B-X$, 2–0 band could not be observed due to the overlap of the intense I^{35}Cl $B-X$, 2–0 band in this energy region.
[c]The transition energies of the linear complexes are that of the most intense peaks, since accurate simulations of these features were not successful.

formed using computer programs obtained from Western[32] and Plusquellic.[33] Initial simulations of the T-shaped bands using both programs qualitatively reproduced the experimental spectra. Once several rotational line assignments could be made, a nonlinear, least squares fitting routine in the Plusquellic program[33] was used to optimize the rotational constants and band origins for each T-shaped He···ICl LIF feature. The fit of the T-shaped He···I^{35}Cl $B-X$, 3–0 band is shown as a gray line in Fig. 5, panel (c), and the spectroscopic constants determined for each of the T-shaped He···$I^{35,37}$Cl bands observed are listed in Table I. The ground and excited state rigid-rotor constants determined from analysis of the T-shaped He···I^{35}Cl 2–0 band agree to within error of the previously reported values,[30] while those of the T-shaped He···I^{35}Cl$(B,v'=3)$ and He···I^{37}Cl$(B,v'=3)$ complexes are reported for the first time. The rotational constants are in accord with near T-shaped structures for both the ground and excited states. A He···ICl(X) Boltzmann rotational temperature of 2.5(3) K was established for each band under these experimental conditions, in agreement with a 2.3(2) K rotational temperature determined by fitting the I^{35}Cl $B-X$, 2–0 rovibronic band. The linewidths of the rotational lines extracted in the fitting of the bands were found to match the resolution of the laser in each of the spectral regions, 0.06 and 0.08 cm^{-1} for the 2–0 and 3–0 spectral regions, respectively. The linewidths yield lower limits on the excited state lifetimes of the T-shaped He···$I^{35,37}$Cl$(B,v'=2)$ and He···$I^{35,37}$Cl$(B,v'=3)$ complexes of 90 and 70 ps, respectively. These observations agree with previous reports, which bracketed the lifetimes of the T-shaped He···I^{35}Cl$(B,v'=3)$ rotor levels between 0.5 and 2.0 ns.[15,18]

The high-resolution LIF spectra of the higher-energy He···ICl features were not successfully simulated nor fit using the rigid-rotor programs[32,33] and converged rotational constants could not be extracted. The shortcomings of the rigid rotor model may arise from Coriolis effects due to the motion of the very light helium atom about the ICl molecule, especially in the excited state. The best simulations using both programs suggest that the ground and excited state structures are not T-shaped, but are more likely linear in both the ground and the excited electronic states. The quality of the simulations is not sufficient to determine if the orientation is He···I–Cl or He···Cl–I, but an orientation of He···I–Cl is the most probable based on comparison with the microwave data for He···ClF (Ref. 5) and considering the higher polarizability of the I atom versus the Cl atom in the ICl moiety. The rigid rotor simulations suggest that the rotational constants would have to increase slightly with electronic excitation in order to exhibit a progression of rotational lines extending to higher energy. An increase in the values of the rotational constants is contrary to the observation of an increased I–Cl bond length, and thus a decreased rotor constant, associated with ICl $B-X$ transitions and of smaller A', B', and C' rotor constants in comparison to the A'', B'', and C'' values for the T-shaped He···ICl(X) complexes in the same spectral region. Another shortcoming of the rigid-rotor simulations of the higher-energy bands is that the simulations consistently predicted fewer rotational lines, especially in the higher-energy region of each feature. It is possible that additional overlapping He···ICl bands with similar rotational contours or fluorescence excitation features of He_n···ICl complexes could contribute to the spectral congestion observed in these regions.

The high-resolution data supports and builds on the conclusions drawn in the previous section. Not only can the spectral features be attributed to two different He···$I^{35,37}$Cl(X) intermolecular levels, but these levels have different equilibrium structures. The most strongly bound, ground state level seems to have a linear He···I–Cl equilibrium structure, although converged rotational constants could not be extracted using the fitting algorithm.[33] Transitions from these levels give rise to the higher-energy He···$I^{35,37}$Cl LIF spectral features within each ICl $B-X$, v'-0 region. The lower energy He···$I^{35,37}$Cl features sample intermolecular vibrational levels with T-shaped structures in both the ground and excited states. Throughout this manuscript, the higher-energy He···$I^{35,37}$ICl features are therefore referred to as linear features and the previously observed features are labeled T-shaped.

The transition energies of the ICl and the He···ICl complexes determined in the ICl $B-X$, 2–0 and 3–0 regions are compiled in Table II. The band origins of the $I^{35,37}$Cl mono-

mer and the T-shaped He···$I^{35,37}Cl$ complex rovibronic transitions represent the values determined from fitting the rotational structure of the respective features and on the calibration of the spectra to the iodine LIF spectra that were recorded concurrently. Since fits of the linear He···ICl features were not achieved, the transition energies represent approximate values. The band origins presented in Table II supersede those extracted from the low-resolution spectra presented above. The high-resolution LIF data also indicate the differences in the binding energies for the ground and excited state intermolecular vibrational levels sampled by each of the He···$I^{35,37}Cl$ transitions. The T-shaped He···$I^{35}Cl$ features are shifted 3.17 and 3.31 cm^{-1} to higher energy than the $I^{35}Cl(B,v'=2)$ and $I^{35}Cl(B,v'=3)$ band origins. The He···$I^{35}Cl(X,v''=0)$ ground state level with a T-shaped geometry is therefore bound by 3.17 and 3.31 cm^{-1} more than the He···$I^{35}Cl(B,v'=2)$ and He···$I^{35}Cl(B,v'=3)$ excited state levels accessed by these rovibronic bands. Similarly, the T-shaped He···$I^{37}Cl(X)$ complex is 3.44 cm^{-1} more strongly bound than the He+$I^{37}Cl(B,v'=3)$ excited state level populated in the corresponding band. The linear bands are shifted to significantly higher energies from the monomer bands indicating that the linear He···$I^{35,37}Cl(X)$ complexes are more than 14 cm^{-1} more strongly bound than the excited He +$I^{35,37}Cl(B,v'=2,3)$ levels accessed. Direct comparisons of the binding energies of the ground state T-shaped He···$I^{35,37}Cl(X)$ complexes to that of the linear He···$I^{35,37}Cl(X)$ based solely on the experimental data cannot be made at this time.

D. Dispersed fluorescence spectra

Extensive two laser, pump–probe experiments aimed at characterizing the excited state dynamics of the T-shaped He···$ICl(B,v'=2,3)$ complexes were undertaken previously.[15–17,30] It was found that the T-shaped complexes dissociate predominantly into He+$ICl(B,v'$-1) products with an ICl rotational product state distribution that is slightly bimodal. The time scale for the vibrational predissociation of the T-shaped He···$ICl(B,v'=3)$ excited state rotor levels was bracketed between 0.5 and 2.0 ns.[15,18] The vibrational predissociation is fast enough so that $ICl(B,v'=2)$ products are observed even though the lifetime of the excited-state $ICl(B,v'=3)$ moiety within the complex has a lifetime that is on the order of hundreds of picoseconds.[26,27,29]

Dispersed fluorescence experiments were undertaken here to qualitatively compare the vibrational predissociation dynamics of the T-shaped He···$I^{35}Cl(B,v'=2,3)$ excited state complexes with that of the newly observed levels populated by the transitions of the linear He···$I^{35}Cl$ bands. Specifically, emission spectra were recorded with the excitation laser, operating with a resolution of 0.22 cm^{-1}, fixed in wavelength to the peak of the T-shaped and linear He···$I^{35}Cl$ bands in the ICl $B-X$, 3–0 spectral region. A helium backing pressure of 115 psi and $x/d=15$ were used. The emission spectrum following excitation of the $I^{35}Cl$ 2–0 bandhead at 17 664 cm^{-1} was also recorded so that a measure of the vibrational relaxation within the expansion could be determined and so that the spectral features attributed to $I^{35}Cl\,B\rightarrow X$, $2\rightarrow v''$ and $1\rightarrow v''$ vibrational progressions could be unambiguously identified.

Greater than 95% of the emission intensity was observed in the $I^{35}Cl\,B\rightarrow X$, $2\rightarrow v''$ vibrational progression with the remainder being in the $I^{35}Cl\,B\rightarrow X$, $1\rightarrow v''$ bands when exciting the bandhead of the $I^{35}Cl\,B-X$, 2–0 feature. The excited state lifetime of the $I^{35}Cl(B,v'=2)$ rotational levels is on the order of 6 μs and thus in a collision-free environment, fluorescence should be observed only in the $2\rightarrow v''$ vibrational bands. Although these experiments were performed 15 nozzle diameters downstream in the expansion, a fraction of the $I^{35}Cl(B,v'=2)$ molecules collide with He atoms and vibrationally relax to rotational levels within the $I^{35}Cl(B,v'=1)$ state prior to fluorescing. The vibrational bands in the dispersed fluorescence spectra obtained with the dye laser tuned to the peak of the T-shaped and linear He···$I^{35}Cl$ features in the ICl $B-X$, 3–0 spectral region were proportional, within the ~20 signal to noise ratio for the measurements, to those observed when exciting the $I^{35}Cl\,B-X$, 2–0 bandhead. The dispersed fluorescence spectra obtained when exciting the $I^{35}Cl\,B-X$, 1–0 bandhead and the T-shaped and linear He···$I^{35}Cl\,B-X$, 2–0 bands are dominated by the ICl $B\rightarrow X$, $1\rightarrow v''$ vibronic bands with ~5% in the $0\rightarrow v''$ bands. Although the emission spectra were much weaker when exciting the complexes, the relative intensities of the resultant $1\rightarrow v''$ and $0\rightarrow v''$ bands again matched, to within noise levels, the spectra obtained when exciting the bare molecules to the $I^{35}Cl(B,v'=1)$ bandhead.

These results indicate that the excited state intermolecular levels accessed by transitions from both the T-shaped and linear He···$I^{35}Cl(X)$ isomers undergo similar vibrational predissociation dynamics forming primarily electronically excited $I^{35}Cl(B,v'$-1) fragments that in turn fluoresce. This is the fluorescence that is detected with the integration gate positioned at long time, black spectrum in Fig. 1, even though the $ICl(B,v'=3)$ and He···$ICl(B,v'=3)$ rotational levels are short-lived.[26,27,29] The frequency resolution of the spectrometer, ~6 cm^{-1}, obscured information concerning the rotational state population distribution within each vibrational band. Two-laser, pump–probe experiments[15–17,30] are underway in our laboratory that are aimed at measuring the $ICl(B,v)$ rotational product state distributions and at providing a more detailed comparison of the vibrational predissociation dynamics for the T-shaped and linear He···$ICl(B,v')$ complexes.

V. DISCUSSION

The low-resolution LIF spectra recorded in the ICl $B-X$, 3–0 region using varying source conditions indicate that the He···$I^{35,37}Cl$ features arise from transitions from two different ground state levels. The high-resolution data for the ICl $B-X$, 2–0 and 3–0 regions suggest that the equilibrium geometry of the most stable He···$I^{35,37}Cl(X,v''=0)$ level is in a linear orientation while the higher energy He···$I^{35,37}Cl(X,v''=0)$ level is definitively nearly T-shaped. The general picture of the He+$ICl(X,v''=0)$ ground state intermolecular potential energy surface that is formed is a

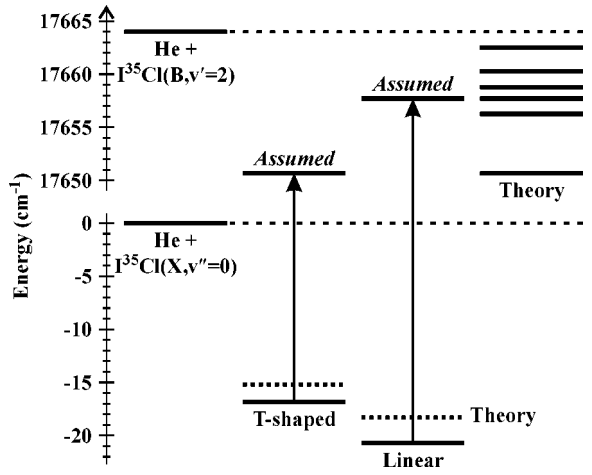

FIG. 6. Energy level diagram for He···I^{35}Cl(X,$v''=0$) and He···I^{35}Cl(B,$v'=2$). The energies of the levels within the excited state on the right-hand side are from the theoretical predictions of Waterland *et al.* (Ref. 18). The ground state energies are determined from the experimentally observed transition energies and from the assumption that the transitions of the T-shaped and linear He···I^{35}Cl(X) complexes access the lowest and second excited intermolecular vibrational levels, respectively, within the He+I^{35}Cl(B,$v'=2$) well predicted by theory. The recently reported theoretical predictions of the ground state binding energies (Ref. 35) dotted lines, are in qualitative agreement with the estimated values.

surface with multiple regions along which the rare gas atom can be localized, resulting in stable linear and T-shaped He···I^{35,37}Cl(X,$v''=0$) isomers. The overall shape of the potential is similar to that accepted for Ar+I$_2$(X,$v''=0$), for which only T-shaped Ar···I$_2$ bands were observed in LIF spectra recorded in the I$_2$ $B-X$ region.[6,7] The ability to see linear He···I^{35,37}Cl intermolecular vibrational bands with rotational structure in the ICl $B-X$, v'-0 LIF spectral region must arise from differences between the He+ICl(B,v') and Ar+I$_2$(B,v') excited state potential energy surfaces and the intermolecular vibrational levels that are bound within these potentials.

Insights into the excited state levels accessed by the transitions in both the T-shaped and linear He···I^{35,37}Cl $B-X$, v'-0 LIF bands can be gained from the theoretical predictions of the He+I^{35}Cl(B,$v'=2$) excited state potential energy surface reported by Waterland *et al.*[18] Pairwise additive interactions were used to model the He+I^{35}Cl(B,$v'=2$) potential and the vibrational decoupling method[34] was implemented to construct the He···I^{35}Cl(B,$v'=2$) eigenfunctions and to determine the bound intermolecular vibrational eigenvalues.[18] The excited state potential has a single minimum in the near T-shaped orientation, as is expected for a potential generated in this manner; specifically, the minimum is located with the He atom at 78.2° from the Cl atom and a He to ICl center-of-mass distance of 3.8 Å and has a depth of 32.5 cm^{-1}. The bound-state calculations determined that six intermolecular vibrational levels are bound within the He +I^{35}Cl(B,$v'=2$) excited state with the lowest $n=0$ level lying 13.3 cm^{-1} below the dissociation limit. The bound intermolecular levels are shown on the right-hand side of the energy level diagram shown in Fig. 6 and are positioned on an energy scale that is relative to the excited state dissociation limit, shown as a dashed line.

The probability density for the lowest He+ICl(B,$v'=2$), $n=0$ level is predicted to be localized in the well region and thus complexes in this level have equilibrium geometries that are nearly T-shaped.[18] The probability density for the $n=1$ level at an energy of -7.7 cm^{-1} from the asymptote is more delocalized in the angular coordinate and has a node at the potential minimum. The $n=2$ second excited intermolecular vibrational level, at -6.3 cm^{-1} from the asymptote, resembles a hindered rotor level with the helium atom sampling a broad range of angles about the ICl molecule. The $n=2$ probability density has a maximum in the linear He···I–Cl geometry, a second slightly lower maximum in the antilinear He···Cl–I geometry, and very little probability density in the nearly T-shaped region. The probability densities for the other three bound vibrational levels were not presented, although it was reported that they each have additional angular nodes with no radial nodes and span wide angular regions of the potential.[34]

The fit of the LIF feature observed at $+3.17$ cm^{-1} from the I^{35}Cl $B-X$, 2–0 monomer transition energy revealed T-shaped He···I^{35}Cl structures for the ground and excited states accessed. Based on comparison with the predicted probability densities,[18] we assign this band to a transition from an energetically excited level within the ground electronic state with a T-shaped average configuration to the $n=0$ lowest energy level lying within the He+I^{35}Cl(B,$v'=2$) excited state. This assignment agrees with that reported in the earlier T-shaped He···I^{35}Cl(B,v') vibrational predissociation dynamics investigations.[17,18,30] The higher energy He···I^{35}Cl feature observed at $+14.3$ cm^{-1} from the I^{35}Cl $B-X$, 2–0 monomer transition energy corresponds to a transition from a ground state level that is more strongly bound than the T-shaped level and which likely has a linear geometry. The best Franck–Condon overlap for a transition from a ground state linear He···I^{35}Cl complex would be to an excited state level with bending excitation, such as the $n=2$ excited state level predicted by Waterland *et al.*,[18] that also has a maximum probability in the linear orientation. Although the excited state surfaces characterizing Rg–dihalogen interactions that are obtained using pairwise additive forces may not be quantitatively accurate, the shapes of the excited state surfaces are simpler than the ground state potentials and pairwise additive potential energy surfaces are often qualitatively accurate.[2] We therefore tentatively assign the higher energy He···I^{35}Cl LIF feature as being a transition from the lowest ground state intermolecular vibrational level with a linear He···I–Cl equilibrium geometry to the $n=2$ second vibrationally excited level within the He +I^{35}Cl(B,$v'=2$) excited state.[18]

A T-shaped He···I^{37}Cl band was not observed in the 2–0 region due to spectral congestion from the I^{35}Cl monomer band. A linear He···I^{37}Cl band was observed at a transition energy shifted by $+14.5$ cm^{-1} from the I^{37}Cl $B-X$, 2–0 band origin. Direct comparisons with the linear He···I^{35}Cl band indicate that the linear He···I^{37}Cl band can be attributed to a transition from the lowest intermolecular level in the He+I^{37}Cl(X,$v''=0$) well to an excited intermolecular vibrational level lying within the He+I^{37}Cl(B,$v'=2$) excited state well, perhaps the $n=2$ level.[18] The eigenvalues

and eigenfunctions within the He+$I^{35}Cl(B,v'=3)$ excited state are not expected to be significantly different than those within the He+$I^{35}Cl(B,v'=2)$ well and we tentatively assign the He···$I^{35}Cl$ features at +3.31 and +14.2 cm^{-1} from the $I^{35}Cl\,B-X$, 3–0 band origin as accessing the T-shaped $n=0$ and linear $n=2$ intermolecular levels, respectively. The similar shifts of the He···$I^{37}Cl$ features, +3.44 and +14.3 cm^{-1}, from the $I^{37}Cl\,B-X$, 3–0 band origin indicate that these transitions access the same intermolecular levels within the He+$I^{37}Cl(B,v'=3)$ potential.

These band assignments permit estimates of the binding energies for the intermolecular levels with T-shaped and linear equilibrium geometries within the He+$I^{35}Cl(X,v''=0)$ ground electronic state to be extracted. In Fig. 6, we have fixed the energies of the excited state levels accessed by the T-shaped and linear He···$I^{35}Cl\,B-X$, 2–0 bands to those of the predicted $n=0$ and $n=2$ intermolecular vibrational levels,[18] respectively. The transition energies of each of the He···$I^{35}Cl$ bands then indicate that the T-shaped and linear He···$I^{35}Cl(X,v''=0)$ levels, shown as solid lines in Fig. 6, are bound by ~17 and ~21 cm^{-1}, respectively.

During the preparation of this manuscript, Prosmiti *et al.*[35] published high-level theoretical calculations of the He+$ICl(X,v''=0)$ ground state *ab initio* potential energy surface and the bound intermolecular vibrational energies and eigenfunctions. The potentials were calculated at coupled cluster using single and double excitations with a noniterative perturbation treatment of triple excitations level of theory with an augmented correlation consistent basis set for the helium atom, supplemented with an additional set of bond functions. In addition, a correlation consistent triple zeta valence basis set in conjuction with large-core Stuttgart–Dresden–Bonn relativistic pseudopotential was employed for the iodine atom.

The ground state surface has the strongest attraction in the linear He···I–Cl orientation (−58.62 cm^{-1} at $\theta=0°$), a well in the near T-shaped orientation that is intermediate in depth (−38.96 cm^{-1} at $\theta=110.9°$), and an antilinear He···Cl–I well is slightly more shallow (−38.03 cm^{-1} at $\theta=180°$).[35] The zero-point energy is significant over the entire surface, especially in the linear region of the potential, as expected, resulting in the three lowest energy levels being bound by only 18.29, 15.15, and 12.33 cm^{-1}. The probability densities for these states indicate that the most strongly bound level is localized in the linear He···I–Cl orientation, the next higher level is localized in the near T-shaped geometry, and the third level is predominantly localized in the antilinear He···Cl–I region of the potential. The predicted energies for the two lowest linear and T-shaped He···$I^{35}Cl(X,v''=0)$ states[11] are shown as dotted levels in Fig. 6 and are in remarkable agreement with the ground state binding energies, 21 and 17 cm^{-1}, roughly estimated using the spectral assignments based on the excited state calculations that utilized pairwise additive forces.[18]

VI. CONCLUSIONS

The LIF spectroscopy results reported here reveal features attributable to rovibronic transitions from separately stabilized He···$I^{35,37}Cl(X,v''=0)$ ground state complexes with nearly T-shaped and linear geometries in the $ICl\,B-X$, 2–0 and 3–0 regions. The Franck–Condon windows for rovibronic transitions of these weakly-bound complexes would suggest that different regions of the excited state potential, which has a minimum in the near T-shaped geometry, should be accessed. Transitions from the energetically favored, linear He···$I^{35,37}Cl(X,v''=0)$ complexes most likely reach He···$I^{35,37}Cl(B,v'=2,3)$ excited state levels with intermolecular bending excitation, such as the $n=2$ states with preferred linear orientations.[18] Transitions of the nearly T-shaped He···$I^{35,37}Cl(X,v''=0)$ complexes, in contrast, terminate on the lowest lying $n=0$ He···$I^{35,37}Cl(B,v'=2,3)$ levels with T-shaped equilibrium geometries.

The binding energies for the T-shaped and linear He···$ICl(X,v''=0)$ isomers are estimated to be 17 and 21 cm^{-1}, respectively, based on comparisons with theoretical predictions for the excited state interactions.[18] The recent ground state calculations performed at a high level of theory have predicted comparable binding energies of ~15 and ~18 cm^{-1} for the T-shaped and linear complexes.[35] Pump–probe experiments are underway in our laboratory that should fine tune the binding energy of the most stable He···$I^{35,37}Cl(X,v''=0)$ isomers.

The He+ICl system represents the first Rg–dihalogen system for which transitions of both T-shaped and linear complexes have been observed with rotational resolution when using LIF spectroscopy. This Rg–dihalogen system may lead to further advances in the understanding of intermolecular interactions, unimolecular reaction dynamics, and energy coupling mechanisms. The overall agreement between already published theoretical predictions[18,35] with our experimental results of the ground and excited state intermolecular vibrational energy levels indicate that calculations can qualitatively and perhaps quantitatively complement experimental efforts aimed at interrogating these phenomena. Systematic studies are currently ongoing in our laboratory that are aimed at characterizing the thermodynamic cooling[36] of the He···$ICl(X)$ complexes down to the lowest energy intermolecular vibrational levels of the complex, at comparing and contrasting the rotational product state distributions following vibrational predissociation from T-shaped[17,18,30] and linear He···$I^{35,37}Cl(B,v'=2,3)$ orientations, and at further characterizing the ground state interactions using two-laser, pump–probe spectroscopic methods.

ACKNOWLEDGMENTS

A Research Corporation Research Innovation Award, a Camille and Henry Dreyfus Foundation New Faculty Award, and a David and Lucile Packard Fellowship in Science and Engineering in part supported this research. The authors appreciate M. I. Lester and T. A. Stephenson for valuable discussions concerning their previous work on He+ICl. The authors would also like to thank C. M. Western and D. F. Plusquellic for providing versions of their asymmetric rotor simulation programs that were used in simulations of the He···ICl spectral features.

[1] D. H. Levy, Adv. Chem. Phys. **47**, 323 (1981).
[2] A. Rohrbacher, J. Williams, and K. C. Janda, Phys. Chem. Chem. Phys. **1**, 5263 (1999).
[3] A. Rohrbacher, N. Halberstadt, and K. C. Janda, Annu. Rev. Phys. Chem. **51**, 405 (2000).
[4] W. Klemperer, C.-C. Chuang, K. J. Higgins, A. S. Miller, and H. C. Fu, Can. J. Phys. **79**, 101 (2001).
[5] K. Higgins, F.-M. Tao, and W. Klemperer, J. Chem. Phys. **109**, 3048 (1998).
[6] M. L. Burke and W. Klemperer, J. Chem. Phys. **98**, 1797 (1993).
[7] M. L. Burke and W. Klemperer, J. Chem. Phys. **98**, 6642 (1993).
[8] J. E. Kenny, K. E. Johnson, W. Sharfin, and D. H. Levy, J. Chem. Phys. **72**, 1109 (1980).
[9] A. Burroughs, G. Kerenskaya, and M. C. Heaven, J. Chem. Phys. **115**, 784 (2001).
[10] D. G. Jahn, W. S. Barney, J. Cabalo, S. G. Clement, A. Rohrbacher, T. J. Slotterback, J. Williams, and K. C. Janda, J. Chem. Phys. **104**, 3501 (1996).
[11] M. I. Hernández, T. González-Lezana, G. Delgado-Barrio, P. Villarreal, and A. A. Buchachenko, J. Chem. Phys. **113**, 4620 (2000).
[12] A. Durand, J. C. Loison, and J. Vigué, J. Chem. Phys. **106**, 477 (1997).
[13] D. H. Levy, Annu. Rev. Phys. Chem. **31**, 197 (1980).
[14] J. P. Toennies and K. Winkelmann, J. Chem. Phys. **66**, 3965 (1977).
[15] J. M. Skene and M. I. Lester, Chem. Phys. Lett. **116**, 93 (1985).
[16] J. M. Skene, J. C. Drobits, and M. I. Lester, J. Chem. Phys. **85**, 2329 (1986).
[17] R. L. Waterland, J. M. Skene, and M. I. Lester, J. Chem. Phys. **89**, 7277 (1988).
[18] R. L. Waterland, M. I. Lester, and N. Halberstadt, J. Chem. Phys. **92**, 4261 (1990).
[19] R. C. Weast, *CRC Handbook of Chemistry and Physics*, 66th ed. (CRC, Boca Raton, 1985).
[20] G. V. Calder and W. F. Giauque, J. Phys. Chem. **69**, 2443 (1965).
[21] M. A. A. Clyne and I. S. McDermid, J. Chem. Soc., Faraday Trans. 2 **72**, 2242 (1976).
[22] W. G. Brown and G. E. Gibson, Phys. Rev. **40**, 529 (1932).
[23] M. A. A. Clyne and I. S. McDermid, J. Chem. Soc., Faraday Trans. 2 **72**, 2252 (1976).
[24] M. Siese, F. Bässmann, and E. Tiemann, Chem. Phys. **99**, 467 (1985).
[25] T. J. Slotterback, S. G. Clement, and K. C. Janda, J. Chem. Phys. **101**, 7221 (1994).
[26] C. D. Olson and K. K. Innes, J. Chem. Phys. **64**, 2405 (1976).
[27] R. D. Gordon and K. K. Innes, J. Chem. Phys. **71**, 2824 (1979).
[28] R. D. Gordon and K. K. Innes, J. Mol. Spectrosc. **78**, 350 (1979).
[29] T. Suzuki and T. Kasuya, J. Chem. Phys. **81**, 4818 (1984).
[30] J. M. Skene, PhD. thesis, University of Pennsylvania, 1988.
[31] R. E. Smalley, D. H. Levy, and L. Wharton, J. Chem. Phys. **64**, 3266 (1976).
[32] C. M. Western, TORTOISE, v3.05 (Department of Chemistry, University of Bristol, 1995).
[33] D. F. Plusquellic, JB 95 Spectral Fitting Program, v1.02.4 (National Institute of Standards and Technology, 2001).
[34] N. Halberstadt, J. A. Beswick, and K. C. Janda, J. Chem. Phys. **87**, 3966 (1987).
[35] R. Prosmiti, C. Cunha, P. Villarreal, and G. Delgado-Barrio, J. Chem. Phys. **117**, 7017 (2002).
[36] A. Bastida, J. Zúñiga, A. Requena, B. Miguel, J. A. Beswick, J. Vigué, and N. Halberstadt, J. Chem. Phys. **116**, 1944 (2002).